Revue des Energies Renouvelables Vol. 14 N°3 (2011) 469 - 480

Indoor and outdoor photovoltaic modules Performances based on thin films solar cells

K. Agroui[1*], A. Hadj Arab[2], M. Pellegrino[3], F. Giovanni[3] and I. Hadj Mahammad[4]

[1] Unité de Développement de la Technologie du Silicium, UDTS
2 Bd. Dr. Frantz Fanon, B.P. 140, Alger, Algérie

[2] Centre de Développement des Energies renouvelables, CDER
B.P. 62, Route de l'Observatoire, Bouzaréah, Alger, Algérie

[3] Photovoltaic Laboratory, ENEA, Portici Research Centre
Area Granatello, 80055 Portici, Naples, Italy

[4] Unité de Recherche Appliquée en Energies Renouvelables, URAER,
B.P. 88, ZI, Garaa Taam, Ghardaïa, Algérie

(reçu le 10 Juin 2011 – accepté le 29 Septembre 2011)

Résumé - *Cet article a pour objectif de réaliser les caractérisations électriques et thermiques des modules photovoltaïques (PV) en couches minces de type silicium amorphe triple jonctions (3J: a-Si) et Cuivre Indium Sélénium (CIS). Les tests sont réalisés en milieu naturel et sous éclairement solaire sur le site saharien de l'URAER de Ghardaïa (Algérie), caractérisé par un ensoleillement intense et une température ambiante élevée, aussi bien que sur le site méditerranéen de l'ENEA-Portici de Naples (Italie). Les tests des performances des modules PV ont été réalisés selon des standards internationaux constituant ainsi un test de diagnostic des principales performances en vue d'une éventuelle comparaison avec les données du constructeur. On a utilisé la technique d'analyse par thermographie infrarouge pour déceler l'homogénéité dans la distribution de la température au niveau des cellules solaires du module PV. Les données issues des tests en milieu naturel ont été converties aux conditions standards de test (STC) par l'utilisation de trois méthodes proposées par A.J. Anderson et G. Blaesser, ainsi que les équations issues de la norme internationales CEI 60891. Ces méthodes de translation se distinguent par le type de la technologie de la cellule solaire, le domaine restreint d'application et la gamme de l'éclairement et de la température. Une différence entre les tests in situ et en milieu naturel existe et elle est attribuée à divers facteurs mais essentiellement à la désadaptation de la réponse spectrale entre le module PV et le dispositif de mesure de l'éclairement.*

Abstract - *This paper summarizes the electrical and thermal characterizations of thin film PV modules based on amorphous triple junctions (3J: a-Si) and Copper Indium Selenide (CIS) thin film solar cells. Tests are operated in outdoor exposure and under natural sunlight of URAER located in Saharan region of Ghardaïa (Algeria) as specific desert climate environment, characterized by high irradiation and temperature levels as well as ENEA-Portici located in Naples (Italy) as Mediterranean site. PV modules performance evaluation was performed according to international standard as diagnostic test of data manufacturer. We used the thermal infrared analysis to detect the homogeneity mapping temperature of solar cells in the PV module. Data acquired from Environmental Operating Conditions (EOC) was converted into solar module output characteristics at Standard Test Conditions (STC) by using three method suggested by A.J. Anderson and G. Blaesser as well as the equations already standardized as IEC 60891. Then, based on the investigation results of the conversion equations, these methods of translation are distinguished by the type of solar cell technology and the*

* kagroui@yahoo.fr

application range. A difference between the tests in situ and in natural environment exists, attributed to various factors but mainly to the mismatch between the spectral responses of PV module and the reference solar cell.

Keywords: Thin Films - Photovoltaic Module – Performances – Translation - Standard Conditions.

1. INTRODUCTION

More than 83 % of photovoltaic (PV) solar modules produced, for terrestrial applications, are made from crystalline silicon solar cells. However, in the past two years, thin-film solar modules based on amorphous silicon (a-Si), cadmium telluride (CdTe), Copper Indium Selenide (CIS) and Gallium Arsenide (GaAs) have gained a strong foothold in the world PV market and PV modules thin film technology becomes one of the most promising PV branches modules.

The Advantages of thin film technologies are [1]:

- Savings in material and energy consumption;
- Half number of process steps;
- Large area deposition;
- Simplified materials handling;
- Monolithic integration;
- Energy pay back time;
- Implementation in building industry.

The test sequence of thin film PV module for the design qualification and type approval is described in IEC 61646; light-soaking and annealing are added due to the special features of thin film PV module.

Also, the stability of peak power of thin film PV module before and after long term outdoor exposure is a crucial parameter for the reliability and durability. However, when evaluating PV performances in environmental operating conditions (EOC), for a practical use, it is difficult to create the measurement conditions identical to STC (Irradiation intensity 1000 W/m^2, module temperature 25 °C, Air Mass 1.5).

Therefore, in most cases the PV module output characteristic values measured with I-V curve tracer are converted into STC values based on various methods [2].

This paper summarizes the electrical characterizations of thin film PV modules based on 3J:a-Si and CIS in outdoor exposure of natural sunlight of Ghardaïa site (Algeria). All results are reported to STC conditions by using three methods for comparative study with manufacturer data sheet.

2. PV MODULES DESCRIPTION

The tested PV modules are based on CIS and a-Si triple junction solar cells from Solar Shell and Uni-Solar manufacturers.

The ST40 PV module utilizes thin layer cells made predominately out of the elements copper, indium and selenium.

The multiple-layer CIS solar cells are laminated between a multi-layered polymer back sheet and layers of ethylene vinyl acetate (EVA) for environmental protection, moisture resistance and electrical isolation [3].

The area of each solar cell is 97.5 cm^2. Solar cells are arranged in 42 series connected cells configuration.

The US64 PV-module utilizes the unique triple-Junction thin film silicon solar cells (3J:a-Si). Each solar cell is composed of three semiconductor junctions stacked on top of each other, forming three different sub-cells.

The area of each solar cell is 450 cm2. The solar cells are arranged in 11 × 2 series-parallel configuration strings and encapsulated in UV stabilized and weather-resistant polymers to form PV Laminates [4].

The polymer encapsulation includes at the front side EVA and the fluoro-polymer ETFE. By-pass diodes are connected across each cell, allowing the modules to produce power even when partially shaded or soiled.

3. PV MODULES INDOOR TESTING

The leakage current is measured according to IEC 61215. The apparatus used to perform electrical isolation test is called Hi-Pot test unit. The test is executed at 1000 VDC added to twice the open circuit voltage at STC (600 VDC) for 1 minute.

The leakage current requirement must be less than 50 μA and the insulating resistance greater than 50 MΩ at 500 VDC as the pass criteria. The ST40 PV module pass successfully the Hi-Pot test but not for the US64 PV module due to electric isolation circuit default.

Table 1 summarises PV modules performances prior to any outdoor exposure and established through indoor measurement with sun simulator under standard test condition (STC) as controlled indoor conditions (100 mW/cm^2, AM 1.5, global spectrum, 25°C) using a calibrated SPIRE 240 solar simulator.

Table 1: PV modules performances at STC conditions

PV Module	P_{max} (W)	I_{sc} (A)	V_{oc} (V)	R_S (Ω)	R_{sh} (Ω)	η (%)
ST40	41.1	3.0	23.1	1.7	65.0	9.6
US64	76.7	6.1	21.7	0.9	19.5	7.6

P_{max} : Maximum power; I_{sc} : Short circuit current; V_{oc} : Open circuit voltage:
R_S : Serial resistance; R_{sh} : Shunt resistance; η : PV module efficiency.

The measured PV module maximum power is compared to the manufacturers' rated maximum power, $P_{max,\,rated}$, and the initial guaranteed minimum power, $P_{max,\,IGM}$, or tolerance as described in **Table 2**.

Table 2: PV modules manufacturers' rated maximum power

	ST40 (CIS)	US64 (3j, a-Si)
$P_{max,\,rated}$ (W)	40	64
$P_{max,\,IGM}$ (W)	36	57.6

The US64 PV module has an initial measured P_{max} value at STC higher than the rated power specified by the manufacturer [5]. This is only a guide to the module's

ultimate performance where an expected photo-degradation of about 15 % is given by the manufacturers.

This is due to an increase in defect density from light-induced degradation in amorphous silicon (Staebler-Wronksi Effect). After exposure to light this effect saturates after 8-10 weeks of operation [6].

Temperature coefficients PV module are typically measured by placing PV module on a temperature controlled test fixture, illuminating the PV module with a solar simulator, measuring the PV module current-voltage (I-V) curve over a range of cell temperatures, and then calculating the rate of change of the desired parameter with temperature.

Table 3 summarizes indoor measurements of effective temperature coefficients for a variety of commercially available photovoltaic modules.

Table 3: Reduced PV modules coefficient temperature

PV module	α'_m (%/°C)	β'_m (%/°C)	γ'_m (%/°C)
ST40	0.0884	-0.314	-0.410
US64	0.0825	-0.436	-0.450

In this **Table**, the units for the temperature coefficients have been normalized to 1/°C by dividing the coefficient by the value for the parameter at STC.

The normalized coefficients are more easily applied to different photovoltaic array configurations with different series/parallel combinations of modules.

These coefficients are symbolized by α'_m, β'_m and γ'_m corresponding short circuit current, open circuit current and maximal power of the module.

4. PV MODULE OUTDOOR TESTING IN SAHARIAN CLIMATE

The outdoor measurements were performed in the site of Applied Research Unit in Renewable Energy, 'URAER' of Ghardaïa as specific desert climate environment, characterized by high irradiation and temperature levels. The geographic characteristics of Ghardaïa site are: - North Latitude: 32°36N; - East Longitude: 3°81E; - Elevation from sea level: 450 m; - Sunlight duration in number of days by year: 77 %.

All modules were installed on south facing latitude des test rack as illustrated in Figure 1.

Fig. 1: PV module type US 645 in outdoor exposure

Experiments are carried out using a modern test facility containing a data acquisition system based on Peak Power Measuring Device Tracer (PVPM 2540C) as illustrated in Figure 2.

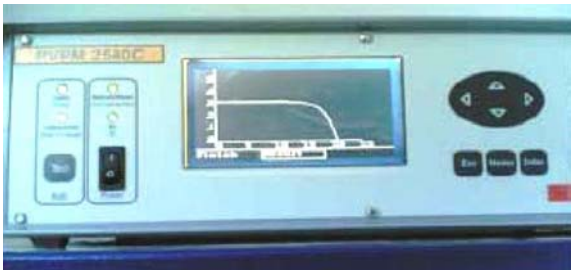

Fig. 2: Representation of experimental set up based on data acquisition PVPM 2540C

The reference solar cell used in our experimental investigation is based on mono-crystalline silicon with integrated Pt 1000 temperature sensor.

Figure 3 shows the evolution of reference cell temperature, ambient temperature and latitude-title irradiance as function of time. During the experiments, the maximal irradiation is 1066 W/m^2, the reference cell temperature is 45°C.

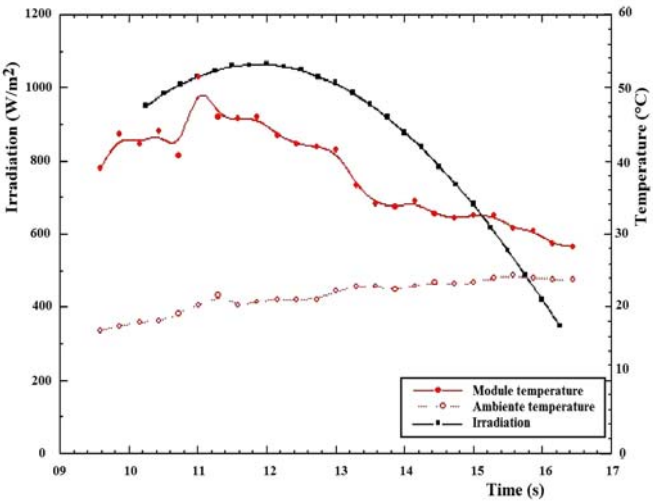

Fig 3: Evolution of reference cell temperature, ambient temperature and latitude-title irradiance as function of time.

Figure 4 shows the correlation between the irradiation and the reference cell temperature at the time of measurements. It is established, for a dry climatic desert condition, that the maximum spectral mismatch error does not exceed, for the natural sunlight on clear days 3 %, if unmatched technology solar cell reference is used as a reference device [7].

The PV modules under test receive an electrical performance (I-V), under environmental conditions for different values of solar irradiance and ambient temperature on a clear sunny day.

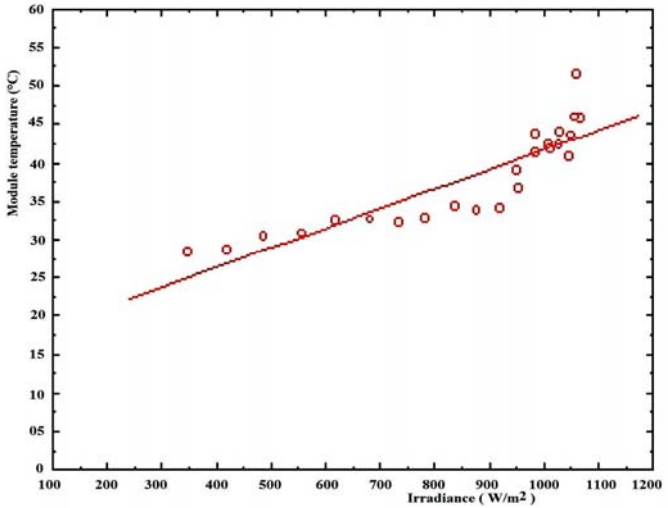

Fig. 4: Correlation between irradiance
and ST 40 PV module temperature

Figs. 5 and 6 show the I-V curves of PV modules ST40 and US64 respectively in environmental conditions EOC.

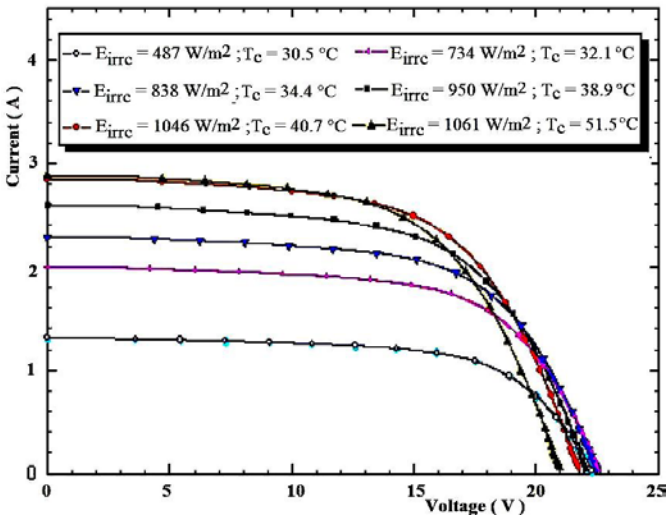

Fig. 5: ST40 PV module I–V characteristics in outdoor testing.

5. CONVERSION METHODS TO STC

Data acquired EOC on a clear sunny day was converted into solar output characteristics in STC by using three conversion methods suggested by J. Anderson [8], G. Blaesser [9] and as well as the equations already standardized as IEC 60891 [10].

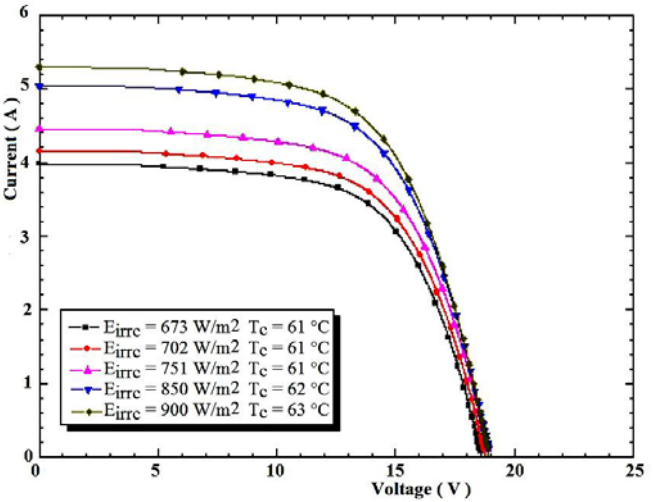

Fig. 6: US64 PV module I– V characteristics in outdoor testing

Only the irradiance dependency coefficient (μ) is deduced from the literature reference [11]. **Table 4** shows the STC conversion equations. From outdoor data, the I-V curves of PV modules under test reported to STC by using conversion methods to STC are represented in Figs. 6 and 7 respectively.

Table 4: STC conversion methods

	I_{sc} Short circuit current
IEC 60981	$I_{sc,2} = I_{sc,1} + I_{sc,EOC} \times (E_2 / E_1 - 1) + \alpha_m (T_2 - T_1)$
Anderson's method	$I_{sc,2} = \dfrac{I_{sc,1}}{[1 + \alpha'_m \times (T_1 - T_2)] \times [E_1 / E_2]}$
Blaesser's method	$I_{sc,2} = I_{sc,1} \times E_2 / E_1 \times (1 + \alpha'_m (T_2 - T_1))$
	V_{oc} Open circuit voltage
IEC 60981	NO equation available for the direct comparison
Anderson's method	$V_{oc,2} = \dfrac{V_{oc,1}}{[1 + \beta'_m \times (T_1 - T_2)] \times [1 + \mu \times \ln(E_1 / E_2)]}$
Blaesser's method	$V_{oc,2} = V_{oc,1} \times (1 + D_v)$ $D_v = \delta \, \mathrm{Ln}(E_2 / E_1) + \beta'_m \times (T_2 - T_1)$
	I – V curve
IEC 60981	$V_2 = V_1 - \beta_m \times (T_2 - T_1) - R_s \times (I_1 - I_2) - K(T_2 - T_1)$ $I_2 = I_1 + I_{sc,1} \times (E_2 / E_1 - 1) + \alpha_m (T_2 - T_1)$

Anderson's method	$V_2 = V_1 \times \left(V_{oc,2} \,/\, V_{oc,1} \right)$ $I_2 = I_1 \times \left(I_{sc,2} \,/\, I_{sc,1} \right)$
Blaesser's method	$V_2 = V_1 + DV + R_s \times (I_1 - I_2)$ $DV = V_{oc,2} - V_{oc,2}$ $I_2 = I_1 \times \left(I_{sc,2} \,/\, I_{sc,1} \right)$

P_{max}, Maximum power

IEC 60981	NO equation available for P_{max} comparison
Anderson's method	$P_{max,2} = P_{max,1} \times E_2/E_1 \times \frac{1}{\left[1 + \gamma'_m (T_2 - T_1)\right]} \times \frac{1}{\left[1 + \mu \ln(E_2/E_1)\right]}$
Blaesser's method	$P_{max,2} = FF_2 \times V_{oc,2} \times I_{sc,2}$ $FF_2 = FF_1 \times (V_{mp,2} \,/\, V_{mp,1})$

Range of application

IEC 60981	Crystalline; Irradiance 700 W/m^2 ; Module temperature: 15 – 35 °C
Anderson's method	Crystalline-Amorphous; Irradiance 100 - 1000 W/m^2 Module temperature: 25 - 75°C
Blaesser's method	Crystalline Irradiance ≥ 600 W/m^2

Where the table nomenclature is described as: E : irradiance; T : Temperature; FF : Fill factor; R_S : Module serial resistance; K : Curve compensation factor; α : Reduced temperature coefficient of I_{sc} ; β : Reduced temperature coefficient of V_{oc} ; γ ': Reduced temperature coefficient of P_{max} ; μ : Irradiance dependency Coefficient.

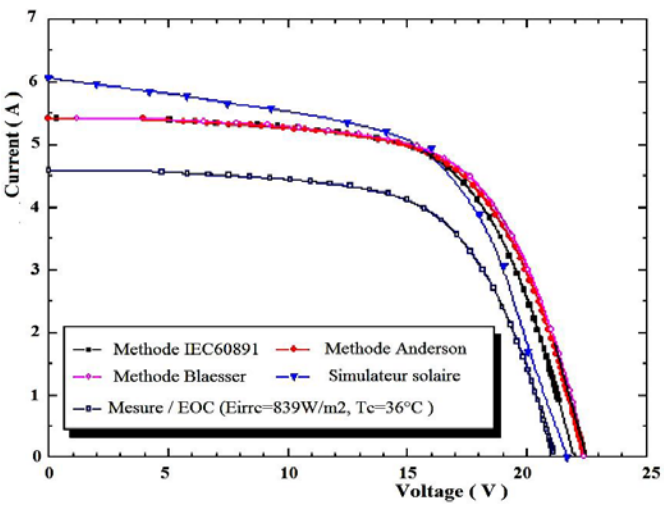

Fig. 7: I-V curve of US64 PV module reported to STC conditions based on conversion methods

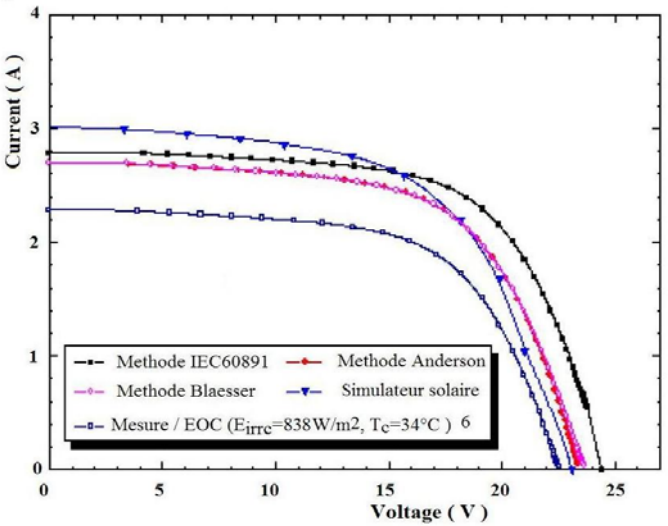

Fig. 8: I-V curve of ST40 PV module reported to STC conditions based on conversion methods

The results of the translation are summarized in **Table 5**.

Table 5: PV module maximum power translated to STC conditions

	Maximum power of ST40 module (W)	Maximum power of US64 module (W)
Under EOC	32.5	62.5
CEI 6089	44.2	79.4
J. Anderson	39.8	78.24
G. Blaesser	39.8	79.4
Solar simulator	41.1	79.1

The ST40 PV module (CIS) has an initial P_{max} value which is essentially equal to its rated value. The deviation of maximum power is 7.5 %, 3.1 % and 3.1 % by using the IEC 60891, A.J. Anderson and G. Blaesser methods respectively.

For US64 PV module, the deviation of maximum power is 0.4 %, 1 % and 0.4 % by using the IEC 60891, A.J. Anderson and G. Blaesser methods respectively.

This is due to the fact that the conversion to the STC values with IEC 60891 method has a limitation in the range of application (crystalline solar cell material, irradiance > 700 W/m^2 and module temperature < 35 °C).

The Deviation includes various factors that lower solar module output such as: effects of spectral changes over time, module temperature, effects of reflection by PV incident angles, effects of solar spectrum according to measurements conditions [12].

6. AMORPHOUS PV MODULE AGEING IN MEDITERRANEAN CLIMATE

6.1 PV module performances evaluation

Figure 9 shows the IV characteristics of US64 PV module under STC after ten years of continuous exposure on ENEA Portici site as Mediterranean climate.

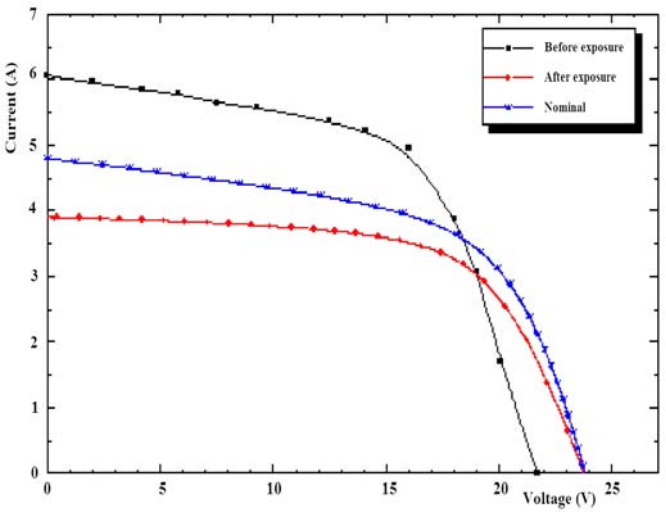

Fig. 9: I-V curve of US64 PV before and after ageing at STC conditions

From the **Table 6**, we note that the maximum power is 58.9W where the annual degradation rate by Staebler-Wronski effect is 0.79 % [13].

Thus, the US64 PV module has a good stability in natural environments [14, 15]. On the other hand, the shunt resistance after exposure was 72.2 Ω while its initial value was of 19.5 Ω.

Thus, the photo-degradation has lead to an increase of the shunt resistance US64 clearly visible on the IV characteristics of the module (stabilization of the amorphous silicon). The serie resistance of PV module is 0.87 and 1.1 Ω before and after exposure respectively.

Table 6: PV modules US64 performances before and after exposure at STC conditions

	P_{max} (W)	I_{sc} (A)	V_{oc} (V)	FF (%)	η_2 (%)
Before exposure	76.6	6.06	21.7	58.3	6.7
After exposure	58.9	3.92	23.8	63.3	5.8

6.2 PV module thermography analysis

The purpose of this test is to determine the ability of the module to withstand the effects of localized heating due for example to a fault in the solar cell (cells

incompatible bad interconnect, short circuit ...) or the deterioration of the encapsulant by using the principle of thermal imaging based on an infrared camera as a non-destructive analysis technique.

Generally a photovoltaic module at 50°C emits heat mainly in the range of wavelengths from 3-20 µm with peak emittance at about 9 µm [16].

The infrared camera used in this work is the Avio TVS 700 type. The thermal image acquisition is realized with the Goratec thermography 2003 software.

The purpose of this polarization by external voltage source is to induce current conduction of solar cells. The temperature profile is obtained by a straight horizontal line across the middle of each string of the PV module.

Figure 10 shows the infrared thermography image and temperature profiles of US64 PV module under a bias current of 5.5, the ambient temperature of the experiments is 30 °C. The US64 PV module has a low temperature of 14.7 °C and a high temperature of 45.2 °C.

The homogeneity in temperature distribution across the PV module is affected due to the photo degradation effect in outdoor exposure.

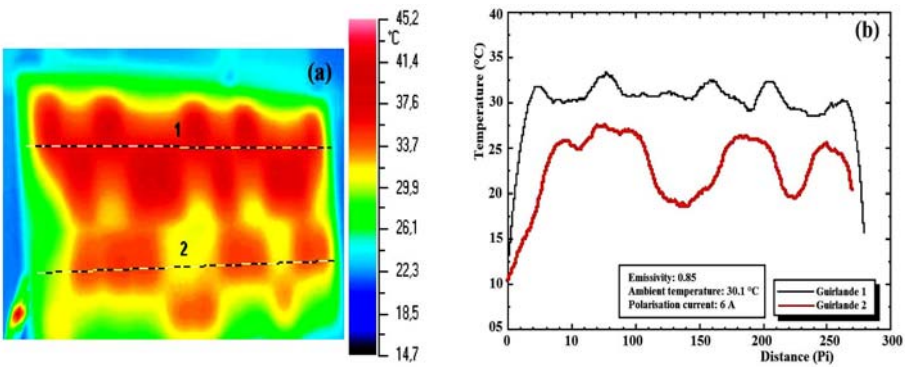

(a) Temperature mapping (b) Temperature profile

Fig. 10: Infrared image of US64 PV module under forward polarization

7. CONCLUSION

These tests have shown that the STC values quoted by manufacturers for their amorphous PV modules do not necessarily match those observed in STC measurements.

So far the measured maximum power values have remained within the values guaranteed by the manufacturers. No significant differences were found among the conversion equation methods in P_{max} deviation with ST40 PV module (CIS).

For US64 PV module (3j: a-Si) the deviation was more varied with the IEC 60891 method than the J. Anderson and G. Blaesser methods. The degradation of amorphous PV module in environmental conditions is due to the Staebler-Wronski effect of the amorphous silicon material structure.

ACKNOWLEDGMENTS

The authors would like to express their gratitude to Dr F. Chenlo from CIEMAT, Spain, for his valuable technical assistance during Algeria-Spain cooperation project.

REFERENCES

[1] A. Boudghene Stambouli, '*Thin-Film Solar Cells and Solid Oxide Fuel Cell Technologies for a Low Cost, Environmentally Friendly and Sustainable Source of Energy*', Proceedings of the International Conference on Renewable Energy, Bejaia, Algeria, November 2007.

[2] H. Nakamura, T. Yamada and T. Ohshiro, '*Comparison Between Estimation for I-V Curve in STC*', Proceedings in the 2nd World Photovoltaic Solar Energy Conference, Vienna, Austria, July, 6-10, 1998.

[3] Y. Tang, G. TamizhMani, L. Ji and C. Osterwald, '*Outdoor Energy Rating of Photovoltaic Modules: Module Temperature Prediction and Spectral Mismatch Analysis*', Proceedings of the 20st European Photovoltaic Solar Energy Conference, Barcelona, Spain, pp. 2051 – 2054, 6-10 June, 2005.

[4] Information on: http://www.uni-solar.com.

[5] A.J. Carr and T.L. Pryor, '*A Comparison of the Performance of Different PV Module Types in Temperate Climates*', Solar Energy, Vol. 76, N°1-3, pp. 285 – 294, 2004.

[6] A. Luque and S. Hegedus, '*Handbook of Photovoltaic Science and Engineering*', Ed. 2003, John Wiley & Sons Inc.

[7] Information on: http://www.socal-solar-energy.com.

[8] Report IEC 60891, '1987', '*Procedures for Temperature and Irradiance Corrections to Measured I-V Characteristics of Crystalline Silicon Photovoltaic Devices*', Amendment 1, 1992.

[9] A. Anderson, '*Photovoltaic Translation Equation: A New Approach*', Final Subcontract Report, NREL/TP-411-20279, January 1996.

[10] G. Blaesser, '*On-Site Power Measurements on Large PV Arrays*', Proceedings of the 10th European Photovoltaic Solar Energy Conference, Lisbon, Portugal, 8-12 April, 1991.

[11] B. Marion, B. Kroposki, K. Emery, J. del Cueto, D. Myers and C. Osterwald, '*Validation of a Photovoltaic Module Energy Ratings Procedure at NREL*', Disponible sur 'http://www.osti.gov/bridge/servlets/purl/909196-OO9pjo'.

[12] R.P. Kenny, A. Ioannides, H. Müllejans, W. Zaaiman and E.D. Dunlop, '*Performance of Thin Film PV Modules*', Thin Solid Films, Vol. 511 – 512, pp. 663 – 672, 2006.

[13] M. van Cleef, P. Lippens and J. Call, '*Superior Energy Yields of UNI-SOLAR Triple Junction Thin Film Silicon Solar Cells Compared to Crystalline Silicon Solar Cells under Real Outdoor Conditions in Western Europe*', Proceedings of the 17th European Photovoltaic Solar Energy Conference and Exhibition, Munich, Germany, 22-26 October, 2001.

[14] A. Gregg, R. Blieden, A. Chang and H. Ng, '*Performance Analysis of Large Scale Amorphous Silicon Photovoltaic Power Systems*', Proceedings of the 31st IEEE Photovoltaic Specialists Conference and Exhibition, Lake Buena Vista, Florida USA, pp. 1615 – 1618, January 3-7, 2005.

[15] C. Radue and E.E. van Dyk, '*Pre-deployment Evaluation of Amorphous Silicon Photovoltaic Modules*', Solar Energy Materials and Solar Cells, Vol. 91, N°2-3, pp. 129 - 136, 2007.

[16] D.L. King, J.A. Kratochvil, M.A. Quintana and T.J. Mc Mahon, '*Applications for Infrared Imaging Equipment in Photovoltaic Cell, Module and System Testing*', Proceeding of the 28th IEEE Photovoltaic Specialists Conference, Anchorage, Alaska, pp. 1487 – 1490, September 15-22, 2000.